

# Medical Image Registration by Normalized Mapping

Qi Wang<sup>a,b</sup>, Cuiming Zou<sup>c</sup>, Lu Yu<sup>a</sup>, Yuan Yuan<sup>a</sup>, Pingkun Yan<sup>a</sup>, Hongbing Lu<sup>d</sup>, Xuelong Li<sup>a</sup>

<sup>a</sup>*Center for OPTical IMagery Analysis and Learning (OPTIMAL), State Key Laboratory of Transient Optics and Photonics, Xi'an Institute of Optics and Precision Mechanics, Chinese Academy of Sciences, Xi'an 710119, Shaanxi, PR China*

<sup>b</sup>*School of Electronic and Control Engineering, Chang'an University, Xi'an 710064, Shaanxi, PR China*

<sup>c</sup>*Faculty of Mathematics and Computer Science, Hubei University, Wuhan 430062, Hubei, PR China*

<sup>d</sup>*Fourth Military Medical University, Xi'an 710032, Shaanxi, PR China*

---

## Abstract

A new non-rigid registration method is proposed for the bladder magnetic resonance (MR) images. The key point is normalized mapping, which transforms any image into an intermediate space. Under the uniform space, those anatomical feature points of different images are corresponded by rotating and scaling. In addition, the non-rigid registration is utilized under the application of groupwise registration. By registering a set of images, an unbiased template can be obtained. Based on this template, the analysis towards the group of images can be easily conducted. Experimental results demonstrate that the proposed method can register accurately the target image to the reference image.

*Keywords:* Non-rigid registration, MR image, normalized mapping, groupwise registration, manifold learning

---

## 1. Introduction

The bladder cancer, widely spread in the world, is the most common malignancy of urinary system and the fourth high-risk cancer in men especially.

---

*Email addresses:* crabwq@opt.ac.cn (Qi Wang), zoucuiming@opt.ac.cn (Cuiming Zou), luyu921@opt.ac.cn (Lu Yu), yuanyuan@opt.ac.cn (Yuan Yuan), pingkun.yan@opt.ac.cn (Pingkun Yan), xuelong\_li@opt.ac.cn (Xuelong Li)

Taking the United States for example, there are approximately 60,240 new cases of bladder cancer per year and 12,710 deaths of them [1] are caused. In order to get a better understanding of bladder cancer, it is necessary to study the bladder structure in more details and get the statistic data on the area of bladder morbidity. Consequently, the analysis of bladder images, such as *MRI*, *CT*, *DSA*, *PET*, and so on, has attracted significant attention in the diagnosis and treatment. Among the techniques employed, one of the most important pre-treated processes is *image registration*. For example, when calculating the cumulative dose delivered in fractionated radiation therapy, there should be a consistent mapping of anatomical structure points between one fraction and another. But there are always changes of locations and shapes. In this case, an accurate registration result is the insurance of an effective radiation therapy [2], [3].

*Registration* is a basic task in image analysis. It means that two or more images are aligned by finding a transformation that minimizes certain distance between the transformed *target images* and the *reference images*. Taking a pair of images for example, image registration means to estimate a mapping between the two images. One image is assumed to remain stationary, which is regarded as the *reference image*, while the other *target image* is spatially transformed to match it [4], [5], [6], [7], [8]. In order to transform the target image to match the reference one, it is necessary to determine a mapping from each position in the reference image to a corresponding position in the target image. It is one of the key steps not only in bladder registration, but also in the registration of other organs. Besides, with the development of medical image technology, the data sets are becoming too large to analyze in practice, for which the *pairwise registration* between two images appears to be inadequate. Consequently, more effective registering methods are being developed for large sets of images, which is regarded as *groupwise registration*. In this paper, a non-rigid registration is proposed and it is utilized under the framework of pairwise and groupwise registration.

### 1.1. Related Work

There are vast literatures on medical image registration during the past decades [9]. *Firstly*, according to the mechanism and the used methodology, existing methods can be generally categorized into *rigid registration* and *non-rigid registration*.

*Rigid registration* has been developed for faster and more robust registration over the past years. The key point for rigid registration is to find

the rotations and translations that optimize some cost functions [10], [11], [12]. There are two kinds of rigid registrations. One of them is between the same modality, such as the images of MR and CT. The other one is between different modalities, such as the images between the above types. The rigid registration between the same modality generally match themselves by minimizing the *mean square error* (MSE) or *mutual information* (MI) [13]. As for different modalities, the aligning is more complex.

Though there has been a large number of accurate and robust methods for rigid registration, in many cases it cannot satisfy the need for clinical experiments. The rigid registration is under the assumption that the interesting anatomical structures do not distort [14]. The assumption not only simplifies the registration process, but also leads to a limited applicability. With the rapid development of registration techniques, the non-linear deformation can be tackled. Then a number of non-rigid registration methods, such as *polynomial based model*, *spline based model*, *elastic model*, *viscous fluid model*, *optical flow model*, and so on, have been proposed to solve this problem.

*Non-rigid image registration* techniques normally either assume an initial rigid body or affine transformation, or are run after a rigid-body or affine algorithm has provided a starting estimate [14]. The thin-plate splines by Bookstein [15], which comes from the availability of the point landmarks, is among the earliest transformations. Meyer *et al.* [16] use the interpolating thin-plate splines to accomplish the non-rigid deformation of the points marked in the moving image. Instead of relying on thin-plate splines, Rueckert *et al.* [17] apply the B-spline to model those deformations. After that, a lot of non-linear registration methods are developed. Lately, Passera *et al.* [18] make comparison of parametric maps generated from tracer kinetic modeling between *Dynamic Contrast Enhanced Computed X-ray Tomography* (DCE-CT) and *Dynamic Contrast-enhanced Magnetic Resonance Imaging* (DCE-MRI) dataset of the bladder images. So *et al.* [19] propose a non-rigid method, which is based on the technique of graph cut in registration. Nevertheless, it is time consuming to deal with the large number nodes for graph cut, although the adoption of multi-level graph cuts can achieve a speed improvement in comparison to a single level graph cut. In order to reduce the computation burden, Weibel *et al.* [20] develop a sparse graph cut based endoscopic bladder image registration method by reducing the number of nodes in the constructed graph while minimizing the loss of information. Besides these techniques mentioned above, other approaches are proposed,

which are based on surface mapping method. Xiong *et al.* [21] propose a method based on finite element analysis. They guide the registration process by three landmarks and establish the correspondence between the meshes of bladder surface.

*Secondly*, the other popular category is based on the scale of the involved images. According to this, existing methods can be classified into *pairwise registration* and *groupwise registration*.

*Pairwise registration* is the mostly developed registration methods. It registers a target image to a reference image for normalization. All of the methods mentioned above are suitable for pairwise registration. Specifically, for the pair of images, one of them is the reference image (sometimes it is called *template*), and the other is the target image. The task is to seek a transformation that corresponds each pixel in the target image to one specific pixel in the reference image.

On the other hand, with the development of imaging and storage technologies, more imaging data need to be analyzed, which demands more effective methods to register large number of images [22]. To this end, *groupwise registration* is proposed to register a set (more than double) of images simultaneously. By registering all of the images simultaneously, the groupwise registration is able to achieve registration consistently and accurately [23], [24], [25], [26]. Based on the work of Wang *et al.* [22], vast modified methods have been proposed to align all subjects simultaneously. Joshi *et al.* [27] propose to register all images to the constructed mean image. In the work of Shattuck *et al.* [28], groupwise registration can be achieved by going around all possible subject combinations of pairwise registrations, which leads to heavy computation cost. Miller *et al.* [29] propose a transitional space to the related objectives by minimizing the sum of all images. Zollei *et al.* [30] successfully apply Miller's method to groupwise registration. They use the stochastic gradient descent and affine transformation for an optimization problem. Balci *et al.* [31] extend Miller's method to non-rigid image registration. They represent the transformations of image by free-form deformations, which is based on the method of B-spline. Although the reference image can be selected in different ways according to the specific problems, the selection of the reference image is mostly subjective, which bring in unavoidable bias to the following process of image analysis [27].

### 1.2. The proposed method

Existing works for registering organs such as brain, heart, and bone abound in a large amount of literatures [9]. But approaches for bladder registration are not so abundant. Direct employment of rigid registration techniques is not suitable because the bladder is not a rigid object and its shape changes much more than other organs with an irregular pattern. Previous non-rigid registration techniques [20], [18] which are often complex, can not necessarily tackle this problem well either since the shape variance is too large. Based on these considerations, a non-rigid registration method is proposed in this paper by utilizing the specific characteristics of bladder. This new method is competent for the pairwise registration of bladder images. Different from existing works that directly manipulating the two images, the presented one registers them through an intermediate space that is normalized to a round shape. This makes the process simple and effective. An application of groupwise registration is also utilized to obtain an unbiased template for the group of images. To do this, a hierarchical strategy, which is based on manifold learning and clustering, is employed to obtain the unbiased template explicitly.

The rest of this paper is organized as follows. Section 2 introduces the proposed method in details, which mainly presents the process about the transformation. Section 3 applies the proposed method to a framework of groupwise registration. Section 4 presents experimental results. In Section 5, discussion and future perspective of this registration study is given.

## 2. Non-rigid image registration

According to the research in *Health Communities* [1], the bladder cancer may be confined to the bladder lining or can extend beyond the lining to surrounding tissues, but the main influence comes from the lining of bladder itself. It suggests that a better study of bladder cancer might be based on the separation of bladder from other tissues in the bladder image. The process of separating bladder from other tissues is regarded as *segmentation*. After the bladder is separated, registration can be done effectively. Normally, registration means to determine a transformation, which corresponds the position of features in one image or coordinate space to the position of the corresponding features in another image or coordinate space [22]. The registration will succeed only if all of the particular positions accurately correspond to the reference one. There are many ways to achieve this objective.

In this paper, a normalized mapping is utilized to perform this task, which also provides an uniform framework for other organs with a similar structure to bladder. Compared with other methods, though the proposed one is simple and straightforward, it is effective and robust.

A brief introduction to the process of non-rigid registration is as follows. Firstly, recall that the examined bladders should be segmented from the original image, one commonly used segmentation method is utilized to get separated bladders. Secondly, the definition of a normalized mapping is presented and the separated bladders are transformed into an uniform shape respectively. Essentially, the uniform shape represents a coordinate system, a different coordinate space from the original one. In this work, a standard circle is utilized to represent the normalized shape. Thirdly, non-rigid registration is carried out under the uniform shape. The details will be discussed below.

### 2.1. Segmentation

With the restriction of medical condition and the particularity of bladder position, existing medical images for bladder study contain both the bladder itself and other tissues. In order to achieve a good performance of registration, the first work of the study is to separate the bladder from other tissues. To this end, a variety of segmentation methods can be employed. In this work, one most widely used method, *Active Shape Models* (ASM) [32], is adopted as an example to segment bladder in the proposed framework.

ASM, developed by Cootes *et al.* [32], is a statistical model for segmentation. The target object is expressed by a set of points, which is constrained by *Point Distribution Model* (PDM) [33]. By incorporating the shape prior information from a set of training images, ASM iteratively transform to match an example of the object in a test image. However, though ASM is a popular segmentation method, it can not achieve the precision segmentation. Additional manual adjustment is also necessary to ensure an accurate result. After this process, those irrelevant and uninteresting organizations are got rid of from the reference and target images by the same PDM model. An example of the target image and the associated segmented part is shown in Fig.1. Those red points are the landmarks involved for segmentation.

### 2.2. Normalized mapping

Since bladders of cancer patients have different pathological changes and shape deformations, it is necessary to transform those bladders into the same

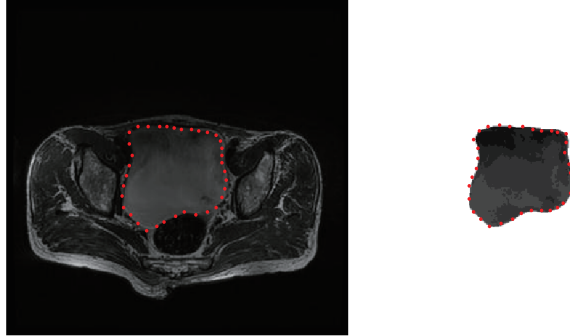


Figure 1: An example of the original image and the corresponding segmented bladder by ASM. The landmarks are shown as red points in the image.

condition, especially in size. As previously described, registration is a transformation essentially, which aims to make the particular positions in an image (or coordinate space) in accordance with those in another image (or coordinate space) [22]. In order to achieve this, a transformation from the original bladder to a normalized space is employed. The normalized space may be any shape, such as a square, rectangle, circle, and so on. In this work, the standard circle is taken as an example. Each bladder is transformed into a minimum circular shape constrained within its circumcircle, on which registration is then conducted. A typical example is illustrated in Fig.2.

Specifically, the boundary of the bladder is projected around the circle, and the area inside the bladder is projected to the corresponding region within the circular shape. The projection is actually a mapping that rays each line segment (from the center of bladder to its boundary, e.g.,  $NE_i$ ) to a radius with a fixed centroid (e.g.,  $OB_i$ ). The center  $N$  of the bladder is automatically estimated as the center of gravity and manually modified by expert if necessary. The length of the radius is the maximum distance between the bladder pixel to the center. It is defined as

$$R = \max_i D(E_i, N), \quad (1)$$

where  $E_i$  is the pixel in the bladder and  $D(, )$  represents the distance between two points. For the calculation of the transformation, a linear mapping is assumed. Taking  $X_i$  and  $Y_i$  for example, the following equation is obeyed

$$\frac{D(X_i, N)}{D(E_i, N)} = \frac{D(Y_i, O)}{D(B_i, O)}. \quad (2)$$

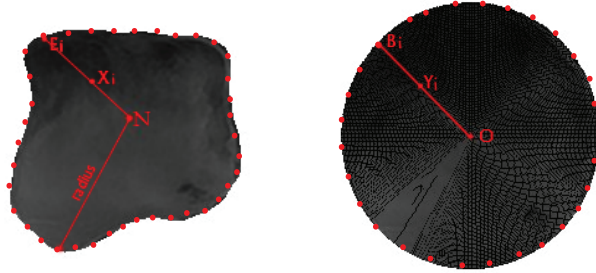


Figure 2: Illustration of normalized mapping. The boundary of the bladder is projected to the boundary around the circle shape while the other points within the bladder are projected to the inner part of the shape.

Another fact should be mentioned is that since the circular shape is larger than the bladder area, there must be holes in the normalized shape as shown in Fig.2. Therefore, an interpolation method is needed to make the intensity of the shape filled. Several interpolation methods exist for this task, such as linear interpolation, nearest interpolation, and *Partial Volume Interpolation*. In the proposed method, the nearest interpolation is adopted and the interpolation result is shown in Fig.3.

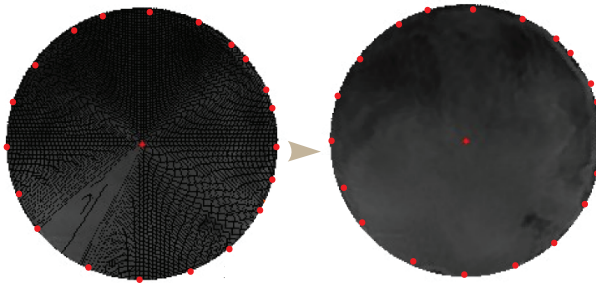


Figure 3: The interpolation process to fill the holes in the transformed circular shape.

### 2.3. Non-rigid registration

In the above subsection, the reference and target images are transformed into a circular shape, respectively. Since different bladder images have different sizes, the obtained circular planes are consequently different in size. This can be found in Fig.4. In order to get the corresponding relationship between the target image and the reference image, the two circular planes should be

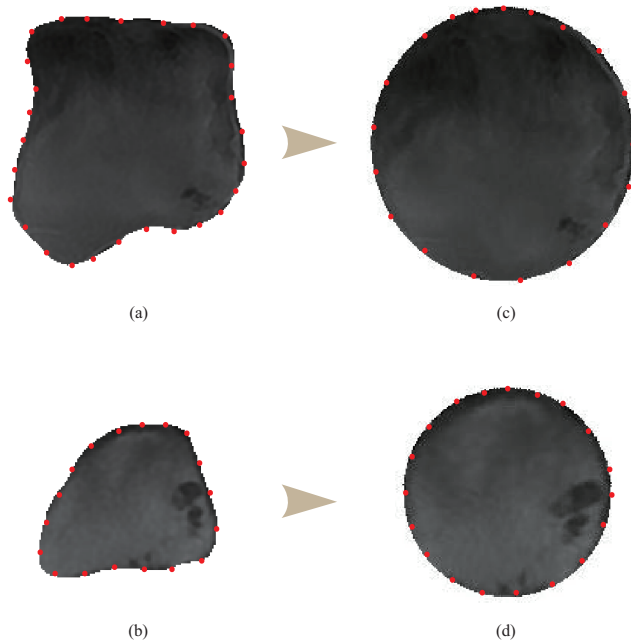


Figure 4: (a) and (b) are the reference image and the target image. (c) and (d) are their corresponding mapping results.

further transformed to the same size. In the following, this nonrigid mapping will be discussed in detail as illustrated in Fig.5.

Given a reference image and a target image, they are respectively transformed into two circular planes as discussed above. Then the smaller one is enlarged to the same size as the larger one. After this process, the two bladders are identical in shape, but their corresponding pixels are not matched correctly indeed. To get a precise match, further adjustment is still needed.

There are two kinds of points in the bladder. One kind of points are around the boundary of the bladder, and the other kind of points are inside the bladder. For the points around the boundary, a registration on the landmarks is first conducted because their positions are known in the ASM segmentation. That means the landmarks in the final segmentation results are ordered and each one represents a corresponding point in the PDM model. Take  $A_1B_1$  and  $A_2B_2$  for example, which are labeled as the landmarks in the original images.  $A_1$  corresponds to  $A_2$  as the identical physiological position and  $B_1$  to  $B_2$ . But after the normalized mapping, the output  $A'_1B'_1$  and  $A'_2B'_2$  are not necessarily in the same place. To establish their correspondence, the

two circular shapes are firstly registered to the same size. Then the position of  $A'_2B'_2$  are adjusted to  $A''_2B''_2$  according to  $A'_1B'_1$  in the circle. By this means, the two pairs of points are corresponded accurately. The points between the landmarks, i.e., arc  $\widehat{A_1B_1}$  and  $\widehat{A_2B_2}$ , are matched linearly according to  $\widehat{A'_1B'_1}$  and  $\widehat{A''_2B''_2}$ . For the points such as  $M$  and  $P$  within the sector, their correspondence is similarly established through an affine transformation. With these obtained correspondence relationships, each pixel in the target image is mapped to one specific pixel in the reference image. The target image is therefore registered to the reference image.

In short, each pixel in the original image is tractable in the transformation. This means for pixels in the target image, its corresponding positions in the reference image can be identified according to the step-by-step transformation. Employing  $\rightarrow$  and  $\leftarrow$  to show the transformation and  $\Leftrightarrow$  to indicate the correspondence relationship, the whole procedure is thus summarized as follows

$$A_1 \rightarrow A'_1 \Leftrightarrow A''_2 \leftarrow A'_2 \leftarrow A_2, \quad (3)$$

$$B_1 \rightarrow B'_1 \Leftrightarrow B''_2 \leftarrow B'_2 \leftarrow B_2, \quad (4)$$

$$M \rightarrow M' \Leftrightarrow P'' \leftarrow P' \leftarrow P. \quad (5)$$

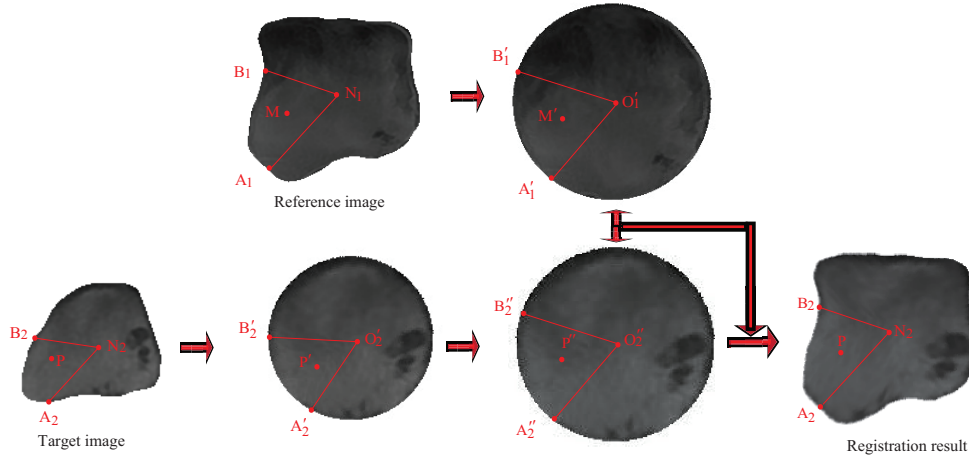


Figure 5: A diagram of the pairwise registration process. Details can be found in the text.

With this explicit correspondence, the target image can be mapped to the reference image. The final registration results are shown in Fig.5.

### 3. Application in groupwise registration

In this section, the proposed non-rigid registration will be unitized in the formwork of groupwise registration. In fact, the groupwise registration can be performed by iteratively utilizing traditional pairwise registration [25], [34]. Several methods have been developed to achieve groupwise registration in this way. For example, Park *et al.* [26] propose to obtain the atlas with the closest image to the real template by performing all pairwise registrations. Nonetheless, this type of methods may be very time-consuming when the dataset is large. Consequently, more effective and faster groupwise registration methods need to be developed. To this end, Joshi *et al.* [27] develop to construct the group mean image first and then registering all images to it, which can improve the computational efficiency. Also, Wu *et al.* [35] propose a hierarchical groupwise registration framework, which breaks down a large-scale groupwise registration problem into a set of small-scale ones. To do this, it first clusters all input images into several classes according to their similarity and then generates the center of each class. Accordingly, the final template can be obtained by applying the atlas synthesis to the above centers. However, it has been shown that in high-dimensional space, Euclidean distance may not appropriately reflect the intrinsic similarity between different images [36], [37]. There have been works addressing the problem in segmentation by manifold learning [36] instead of Euclidean space. But to the best of the author’s knowledge, the usage in groupwise registration has not been seen.

Given a group of bladder MR images, the application is also under the framework of hierarchical groupwise registration [35]. It consists of two main steps: image clustering with manifold learning technique, and non-rigid registration on all the images. Through the groupwise registration, a template image is selected unbiasedly and other images can be registered to it. A diagram is presented in Fig.6 to illustrate the process.

In Fig.6, the first floor is a group of MR images to be registered. These images are in the same size, and each image is segmented by the method discussed in Section 2.1. The obtained bladders are represented by a high-dimensional vector. Since the high-dimensional data is a challenge of the computational and storage ability, and on the other hand, expression in Euclidean space is considered inappropriate compared in manifold space [36], a preprocessing step of dimensionality reduction is therefore needed. Suppose there are  $l$  bladder images and each is denoted by a high-dimensional vector

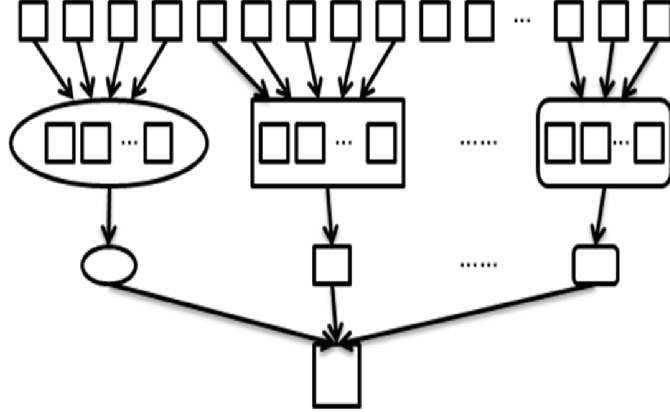


Figure 6: A flowchart of the hierarchical registration.

$\{X_i\}_{i=1,2,\dots,l}$ . Each  $\{X_i\}$  is a concatenated coordinate values of bladder landmarks. In order to reduce the  $m$ -dimensional vector  $X_i$  to  $n$ -dimensional  $Y_i$  ( $m > n$ ), a projection matrix is learned by manifold learning. There are several algorithms available for this task (e.g., LLE, LPP, Isomap [38]). In this application, *Locality Preserving Projections* (LPP) [39] is utilized because of its superior performance. The projection model can be expressed as

$$Y_i = PX_i, \quad (6)$$

where  $P$  stands for the transformation matrix.

After that, K-means clustering is applied to these low dimensional vectors, and the images are classified into  $g$  groups  $\{G_k\}_{k=1,2,\dots,g}$ . The second floor in Fig.6 is the process of clustering. A mean representative is then selected for each group. The representative  $R_k$  for group  $k$  is defined as the image having the minimum Mean Squared Error (MSE) with other ones:

$$R_k = \arg \min_{X_{ki}} MSE(X_{ki}, X_{kj}), \quad (7)$$

where  $X_{ki}$  and  $X_{kj}$  are the images in group  $k$ .

At the bottom of the diagram, the final template  $R_{temp}$  is obtained by averaging the group representatives in a higher level with different weights:  $R_{temp} = \sum_k w_k R_k$ , where  $w_k$  is the weight for group  $k$  and it is proportional

to the number of images within the group. In the end, an unbiased template is obtained and all the images can be registered to the template.

## 4. Experiments

In this section, two experiments are conducted to evaluate the performance of the proposed non-rigid registration method. The first one is pairwise registration on 27 MR images and the second one is groupwise registration on 65 MR images. All the images are  $515 \times 512$  and have bladder tumors with them.

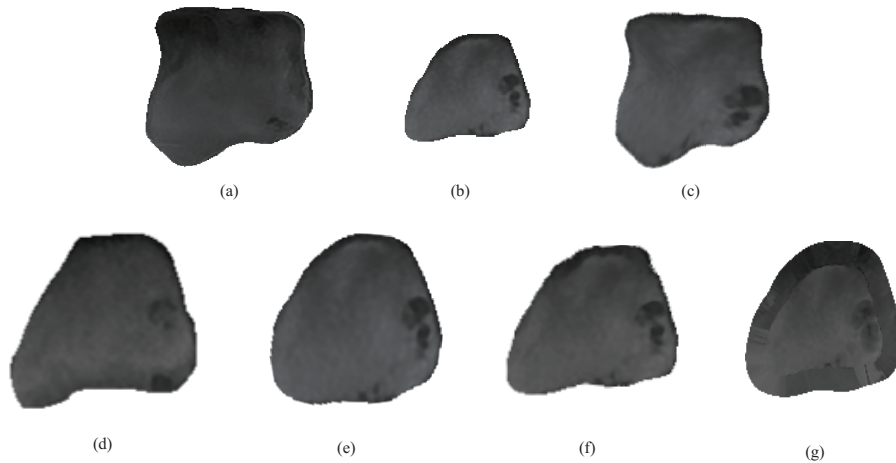


Figure 7: Pairwise registration results. (a) Reference image. (b) Target image. Registration results by the proposed method (c), similarity transform based registration (d), the B-spline based registration (e), deformable registration based on Demons (f) and level set motion (g).

### 4.1. Pairwise registration

In this subsection, the proposed normalized mapping based method is compared with several popular methods representing the state-of-the-art both qualitatively and quantitatively [40]. They are the similarity transform based registration, the B-spline based registration [40], deformable registration based on Demons [41] and level set motion [42]. The pairwise registration is conducted by choosing one image as reference one and the other 26 as target ones. One typical outcome for these methods is displayed in Fig. 7. From the figure, it is clear that the reference image (a) and target image (b)

are different. After pairwise registration, the results of comparative methods are not satisfying because the transformed images are still different from the reference one. But the proposed method performs well because the mapping result is almost the same with the reference one.

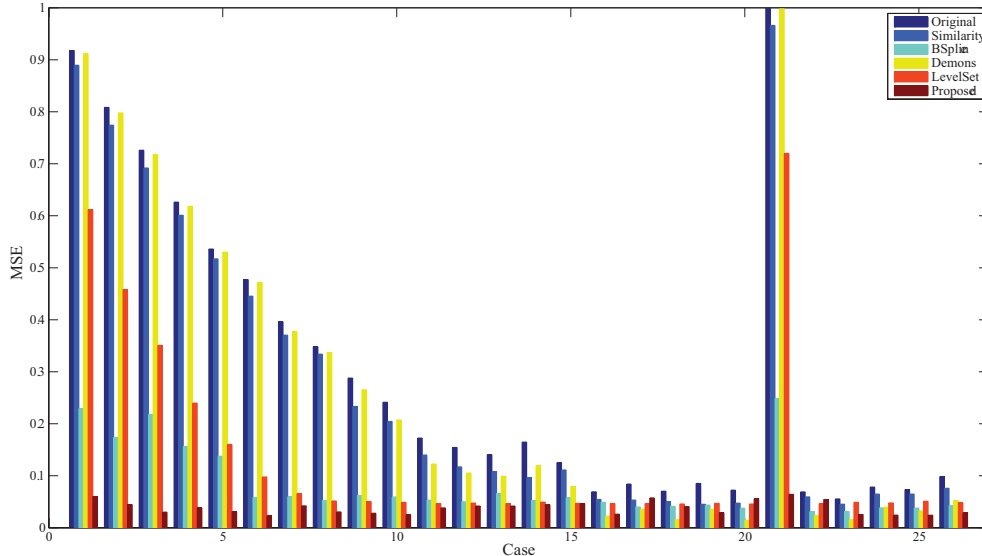


Figure 8: The MSE results for the original image pair before registration, and the image pair after registration by the proposed method and the competitive methods. The horizontal axis represents the 26 image cases registered to the reference image.

In order to quantitatively compare the proposed method with other methods, two evaluation criteria, namely *Mean Squared Error* (MSE) [13] and *Dice Similarity Coefficient* (DSC) [43], are employed. The MSE can reflect the intensity similarity between a pair of images, which is defined as:

$$MSE = \frac{1}{N} \sum_{i=0}^{N-1} (r_i - t_i)^2, \quad (8)$$

where  $N$  stands for the total pixels in the image,  $r_i$  is the pixel intensity of the reference image, and  $t_i$  represents the pixel intensity of the target image. Fig.8 shows the statistical results of registration after normalizing the MSE value to  $[0, 1]$ . It can be seen that the original target images have great dissimilarities compared with the reference ones and their corresponding MSE

values are large. But after registration, their resemblances improve a lot and the MSE values decrease greatly. Compared with other methods, the proposed method achieves better performance. This superiority is much more magnificent especially for images with larger shape variations, which correspond to high original MSE values before registration in Fig.8. Therefore, it is obvious that the proposed method is more effective for the registration of large variation. Nevertheless, the performance for the 17th, 20th and 22th cases appear not conforming to the conclusion. Their MSE values are a little higher than those of other methods. But the differences are less than 0.05 and are hard to identify in the registered images (The shape variation with the reference image after registration is reflected in the DSC measure in the following).

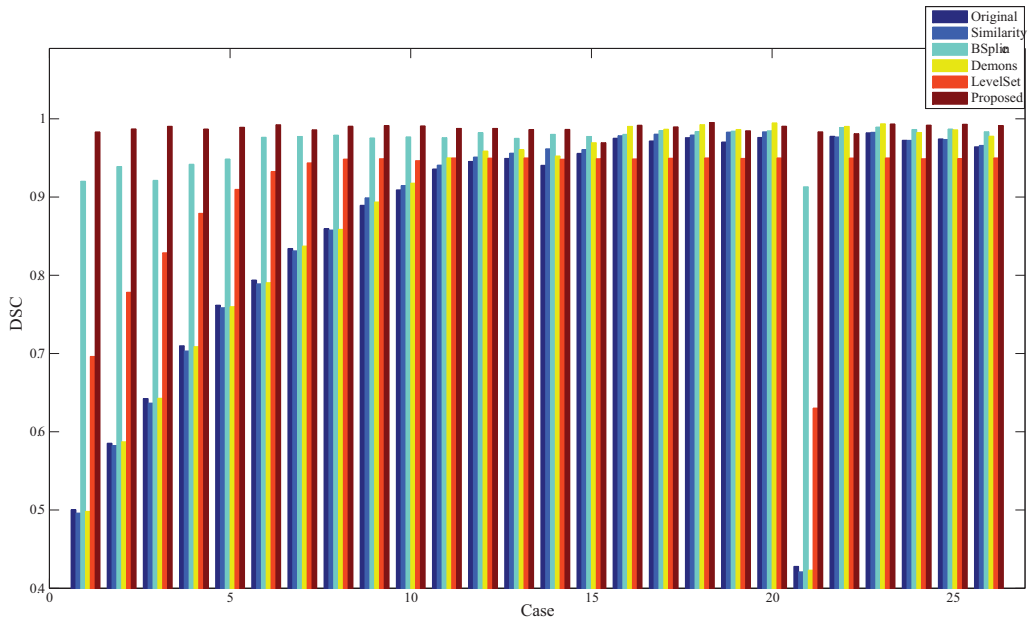


Figure 9: The DSC results for the original image pair before registration, and the image pair after registration by the proposed method and the competitive methods. The horizontal axis represents the 26 image cases registered to the reference image.

The other evaluation criterion is DSC, which is also a widely used similarity measurement in image registration. It reflects the shape correlation

degree between two images [43]. It is defined as:

$$DSC(R, T) = \frac{2|R \cap T|}{|R| + |T|}, \quad (9)$$

where  $R$  and  $T$  represent the reference image and target image, respectively.  $|\cdot|$  denotes the area of the bladder region. The DSC value varies between 0 and 1 and a higher value indicates a better alignment. In Fig. 9, we plot the DSC before registration and after registration by different methods. From the curves it is evident that the proposed method outperforms the other competitive ones, especially when the original image pairs have great shape differences. Besides, the proposed method performs more consistent and robust across various images.

#### 4.2. Groupwise registration

In the following, some experiments are conducted to demonstrate the applicability of the proposed method in hierarchical registration framework. The goal of this section is to estimate the unbiased template for the group of images. A dataset containing 65 MR images of bladder cancer is utilized. These images are pre-treated, in which the bladder parts are segmented by ASM method. The obtained results are then utilized as the input images in the proposed application. As has been mentioned in Section 2, the dimension of the input image data is reduced first by the LPP algorithm and then the data is clustered by classical K-means clustering. After that, representatives is selected from each group and the final template is averaged by an unequal weighting. The detailed process and the results are shown in Fig. 10.

By this means, all the images can be registered to the template and the input images become similar with the comparable anatomical structure. Analysis (such as getting statistics of the tumor location and size) based on this results is easy and straightforward.

## 5. Conclusion

In this paper a novel method for non-rigid registration of bladder MR images is proposed. Different from previous works, the proposed method is based on a normalized mapping, which seeks an intermediate coordinate space to fulfill the registration task. Experiments verify that the proposed method can achieve better performance than other competitive methods.

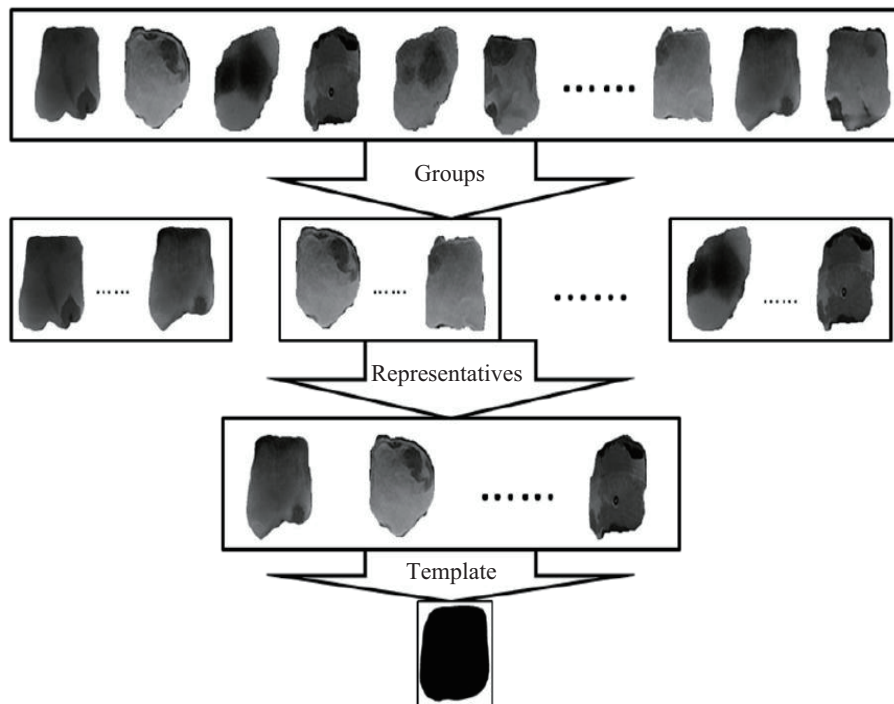


Figure 10: Groupwise registration results. The first level is the input images; the second level is the clustering result; the third level is the representatives selected from each group; and the last level is the final template, which will be used as the reference image by other input images.

Moreover, the proposed non-rigid registration is applied in groupwise registration to obtain the unbiased template, which also illustrates the effectiveness of the proposed method. Nevertheless, apart from the advantages of the proposed method, there are still limitations associated with it. The proposed non-rigid registration method is probably suitable for bladder-like images. It will fail on images like brain structure. For one reason, this kind of structure is hard to be mapped to a normalized shape. For another, the complexity of the structure will lead to inaccurate segmentation and registration, which will require more human intervention. This also makes it impractical. Techniques to overcome these limitations will be developed in our future work.

## References

- [1] R. Levin, S. J. Swierzewski, <http://www.healthcommunities.com/bladder-cancer/overview-of-bladder-cancer.shtml>, 1998.
- [2] L. Xiong, A. Viswanathan, A. Stewart, S. Haker, C. Tempany, L. Chin, R. Cormack, Deformable structure registration of bladder through surface mapping, *Medical Physics* 33 (2006) 1848–1856.
- [3] K. Noe, K. Tanderup, T. Sorensen, Surface membrane based bladder registration for evaluation of accumulated dose during brachytherapy in cervical cancer, in: *IEEE International Symposium on Biomedical Imaging*, IEEE, 2011, pp. 1253–1256.
- [4] B. Fischer, J. Modersitzki, Ill-posed medicine-an introduction to image registration, *Inverse Problems*. 24 (2008) 2003–2023.
- [5] A. Wismüller, F. Vietze, D. R. Dersch, J. Behrends, K. Hahn, H. Ritter, The deformable feature map - a novel neurocomputing algorithm for adaptive plasticity in pattern analysis, *Neurocomputing* 48 (2002) 107–139.
- [6] J. Jiang, J. Cheng, X. Chen, Registration for 3-d point cloud using angular-invariant feature, *Neurocomputing* 72 (2009) 3839–3844.
- [7] H. Liu, J. Yan, D. Zhang, Three-dimensional surface registration: A neural network strategy, *Neurocomputing* 70 (2006) 597–602.
- [8] L. Shang, J. Lv, Z. Yi, Rigid medical image registration using pca neural network, *Neurocomputing* 69 (2006) 1717–1722.
- [9] F. Khalifa, G. M. Beache, G. Gimelfarb, J. S. Suri, A. S. El-Baz, State-of-the-art medical image registration methodologies: A survey, in: A. S. El-Baz, R. Acharya U, M. Mirmehdi, J. S. Suri (Eds.), *Multi Modality State-of-the-Art Medical Image Segmentation and Registration Methodologies*, Springer US, 2011, pp. 235–280.
- [10] N. M. Alpert, J. F. Bradshaw, D. Kennedy, J. A. Correia, The principal axes transformation-a method for image registration, *Nuclear Medicine* 31 (1990) 1717–1722.

- [11] X. Gu, S. J. Gortler, H. Hoppe, Geometry images, *ACM Transactions on Graphics* 21 (2002) 355–361.
- [12] T. L. Faber, E. M. Stokely, Orientation of 3-d structures in medical images, *IEEE Transactions Pattern Analysis and Machine Intelligence* 10 (1988) 626 – 633.
- [13] J. Ashburner, K. J. Friston, *Rigid Body Registration*, Academic Press, London, 2007.
- [14] D. L. G. Hill, P. G. Batchelor, M. Holden, D. J. Hawkes, Medical image registration, *Physics in Medicine and Biology* 46 (2001).
- [15] F. L. Bookstein, Principal warps: thin-plate splines and the decomposition of deformations, *IEEE Transactions Pattern Analysis and Machine Intelligence* 11 (1989) 567 – 585.
- [16] C. Meyer, J. Boes, e. a. B. Kim, Demonstration of accuracy and clinical versatility of mutual information for automatic multimodality image fusion using affine and thin plate spline warped geometric deformations 3 (1997).
- [17] D. Rueckert, L. Sonoda, C. Hayes, D. Hill, M. Leach, D. Hawkes, Non-rigid registration using free-form deformations: application to breast mr images, *IEEE Transactions on Medical Imaging* 18 (1999) 712–721.
- [18] K. Passera, L. Mainardi, D. McGrath, J. Naish, D. Buckley, S. Cheung, Y. Watson, A. Counce, G. Buonaccorsi, J. Logue, M. Taylor, C. Taylor, H. Young, G. Parker, A non-linear registration method for DCE-MRI and DCE-CT comparison in bladder tumors, in: *International Symposium on Biomedical Imaging*.
- [19] R. So, A. Chung, Multi-level non-rigid image registration using graph-cuts, in: *International Conference on Acoustics, Speech and Signal Processing*, IEEE, 2009, pp. 397–400.
- [20] T. Weibel, C. Daul, D. Wolf, R. Röch, A. Ben-Hamadou, Endoscopic bladder image registration using sparse graph cuts, in: *International Conference on Image Processing*, IEEE, 2010, pp. 157–160.

- [21] L. Xiong, A. Viswanathan, A. J. Stewart, L. M. Chin, R. A. Cormack, Deformable structure registration of bladder through surface mapping 33 (2006).
- [22] Q. Wang, L. Chen, D. Shen, Group-wise registration of large image dataset by hierarchical clustering and alignment, in: Medical Imaging, volume 7259, SPIE, 2009.
- [23] B. Zitová, J. Flusser, Image registration methods: a survey 21 (2003) 977–1000.
- [24] W. R. Crum, T. Hartkens, D. L. G. Hill, Non-rigid image registration: theory and practice, British Journal of Radiology (2004) 140–153.
- [25] D. Seghers, E. D’Agostino, F. Maes, D. Vandermeulen, P. Suetens, Construction of a brain template from mr images using state-of-the-art registration and segmentation techniques, in: Medical Image Computing and Computer Assisted Intervention, volume 3216, Springer, 2004, pp. 696–703.
- [26] H. Park, P. H. Bland, A. O. Hero, C. R. Meyer, Least biased target selection in probabilistic atlas construction, in: Medical Image Computing and Computer Assisted Intervention, volume 3750, Springer, 2005, pp. 419–426.
- [27] S. Joshi, B. Davis, M. Jomier, G. Gerig, Unbiased diffeomorphic atlas construction for computational anatomy 23 (2004) 151–160.
- [28] D. W. Shattuck, M. Mirza, V. Adisetiyo, C. Hojatkashani, G. Salamon, K. L. Narr, R. A. Poldrack, R. M. Bilder, A. W. Toga, Construction of a 3d probabilistic atlas of human cortical structures 39 (2008) 1064–1080.
- [29] E. G. Learned-Miller, Data driven image models through continuous joint alignment 28 (2006) 236–250.
- [30] L. Zollei, E. Learned-Miller, E. Grimson, W. Wells, Efficient population registration of 3d data, in: International Conference on Computer Vision, volume 3765, IEEE, 2005, pp. 291–301.

- [31] S. K. Balci, P. Golland, M. Shenton, W. M. Wells, Free-form b-spline deformation model for groupwise registration, in: *Medical Image Computing and Computer Assisted Intervention*, Springer, 2007, pp. 105–121.
- [32] T. Cootes, C. Taylor, D. Cooper, J. Graham, Active shape models: their training and application 61 (1995) 38–59.
- [33] T. F. Cootes, P. Kittipanyangam, Comparing variations on the active appearance model algorithm, in: *British Machine Vision Conference*, volume 1, British Machine Vision Association, 2002, pp. 837–846.
- [34] C. J. Twining, T. Cootes, S. Marsland, V. Petrovic, R. Schestowitz, C. J. Taylor, A unified information-theoretic approach to groupwise non-rigid registration and model building, in: *Information processing in medical imaging*, volume 19, Springer, 2005, pp. 1–14.
- [35] G. Wu, Q. Wang, H. Jia, D. Shen, Groupwise registration by hierarchical anatomical correspondence detection, in: *Medical Image Computing and Computer Assisted Intervention*, Springer, 2010, pp. 20–24.
- [36] Y. Cao, Y. Yuan, X. Li, B. Turkbey, P. L. Choyke, P. Yan, Segmenting images by combining selected atlases on manifold, in: *Medical Image Computing and Computer Assisted Intervention*, Springer, 2011, pp. 272–279.
- [37] J. B. Tenenbaum, V. de Silva, J. C. Langford, A global geometric framework for nonlinear dimensionality reduction, *Science* 290 (2000) 2319–2323.
- [38] L. Cayton, Algorithms for manifold learning, UCSD tech report CS2008-0923 (2005).
- [39] X. He, P. Niyogi, Locality preserving projections, in: *Neural Information Processing Systems*, 2003, volume 16, pp. 153–160.
- [40] L. Ibáñez, W. Schroeder, L. Ng, etc., *The itk software guide* (2008).
- [41] J.-P. Thirion, Image matching as a diffusion process: an analogy with maxwells demons, *Medical Image Analysis* 2 (1998) 243C260.

- [42] S. Osher, R. P. Fedkiw, Levelset methods: An overview and some recent results, *Journal of Computational Physics* 169 (2001) 463C502.
- [43] R. Alterovitz, K. Goldberg, J. Pouliot, I. J. Hsu, Y. Kim, S. M. Noworolski, J. Kurhanewicz, Registration of mr prostate images with biomechanical modeling and nonlinear parameter estimation, *Medical Physics* 33 (2006) 446–454.



**Qi Wang** received the B.E. degree in automation and Ph.D. degree in pattern recognition and intelligent system from the University of Science and Technology of China, Hefei, China, in 2005 and 2010 respectively. He is currently a postdoctoral researcher with the Center for Optical Imagery Analysis and Learning, State Key Laboratory of Transient Optics and Photonics, Xi'an Institute of Optics and Precision Mechanics, Chinese Academy of Sciences, Xi'an, China. His research interests include computer vision and pattern recognition.



**Cuiming Zou** is currently working toward the M.S. degree in the Faculty of Mathematics and Computer Science, Hubei University, Wuhan, China. Her research interests include machine learning, medical image processing, and image processing.

**Lu Yu** is currently working toward the M.S. degree in Xi'an Institute of Optics and Precision Mechanics, Chinese Academy of Sciences, Xi'an, China.

**Yuan Yuan** is a researcher (full professor) with Chinese Academy of Sciences, and her main research interests include Visual Information Processing and Image/Video Content Analysis.



**Pingkun Yan** received the B.Eng. degree in electronics engineering and information science from the University of Science and Technology of China, Hefei, China, and the Ph.D. degree in electrical and computer engineering from the National University of Singapore, Singapore. He is currently a Full Professor with the Center for Optical Imagery Analysis and Learning, State Key Laboratory of Transient Optics and Photonics, Xian Institute of Optics and Precision Mechanics, Chinese Academy of Sciences, Xi'an, China. His research interests include computer vision, pattern recognition, machine learning, and their applications in medical imaging.



**Hongbing Lu** received her PhD degree in Biomedical Engineering from Tsinghua University of China in 1998. After graduation, she had been a post-doctoral researcher in Radiology at State University of New York at Stony Brook for three years. She joined the Fourth Military Medical University in 1991 and currently is a professor and director of the Computer Application Department, BME. Her research interests focus on computer-aided detection and diagnosis, medical image reconstruction, noise reduction, medical application of processing and visualization methods. She has authored more than 60 scientific publications and is the principal investigator of over ten projects funded by the National Science Foundation of China, by Ministry of Science and Technology, and by the Department of Defense.

**Xuelong Li** is a full professor with the Center for OPTical IMagery Analysis and Learning (OPTIMAL), State Key Laboratory of Transient Optics and Photonics, Xi'an Institute of Optics and Precision Mechanics, Chinese Academy of Sciences, Xi'an 710119, Shaanxi, P. R. China.